JGR Space Physics

RESEARCH ARTICLE
10.1029/2020JA028441

Key Points:

- The classic Banks theoretical model underestimates O^+-O collision frequency by 30% at 1000 K
- The correction-factor model is based on the classic model due to a misunderstanding that the classic model is based on laboratory results
- The classic model is corrected by the later wide-energy model, and thus should be replaced by this model

Correspondence to:
Akimasa Ieda,
ieda@isee.nagoya-u.ac.jp

Citation:
Ieda, A. (2021). Atomic oxygen ion-neutral collision frequency models at ionospheric temperatures. *Journal of Geophysical Research: Space Physics*, *126*, e2020JA028441. https://doi.org/10.1029/2020JA028441

Received 15 JUL 2020
Accepted 23 OCT 2020

Atomic Oxygen Ion-Neutral Collision Frequency Models at Ionospheric Temperatures

A. Ieda[1]

[1]Institute for Space-Earth Environmental Research, Nagoya University, Nagoya, Japan

Abstract The collision between atomic oxygen and its first positive ion plays a major role in Earth's F region ionosphere. An accurate corresponding collision frequency model is necessary to quantitatively understand the ionosphere. However, the widely used classic Banks theoretical model typically provides a collision frequency that is 30% lower than the expectation from ionospheric observations. Accordingly, the classic collision frequency is often adjusted by multiplying it by a constant known as the Burnside factor. This correction-factor model adopted the classic model as its basis due to a misunderstanding that the classic model was based on a laboratory experiment; that is, the correction factor was originally meant to compensate for laboratory contamination. In this study, a collision frequency model is constructed based on the laboratory experiment, and the resultant laboratory-based model is found to be consistent with ionospheric observations. In this construction, the impact of laboratory contamination is determined to be small (7%) and is mostly canceled by a misinterpretation regarding the conventional definitions of energy. Thus, the 30% difference is mainly caused by a theoretical error in the classic model itself. This error is energy-dependent and corrected by the later wide-energy theoretical model. Thus, the classic model cannot be corrected by a temperature-independent constant and should be replaced by the later model.

Plain Language Summary Earth's ionosphere is a region at altitudes between 60 and 800 km. The ionosphere includes both neutral atmosphere and plasmas and is thus the interface between Earth and space. The plasma density reaches its maximum at an altitude of about 300 km, where the dominant species are atomic oxygen and its first positive ion. Collisions between this particle pair play an important role in the structure and dynamics of the ionosphere. However, the collision frequency calculated from the widely used classic model has been reported to be about 30% lower than ionospheric observations for unknown reasons. In this study, the major reason for this underestimation is clarified to be that the classic model has adopted a less accurate collision cross-section model. Thus, the classic model should be replaced by the later wide-energy model.

1. Introduction

The O^+-O collision controls the interaction between the neutral atmosphere and the F region ionosphere of the Earth. Its frequency, $\nu(O^+\text{-}O)$, is necessary to calculate the drag force, the electric conductivity, and the ambipolar diffusion. Thus, an accurate $\nu(O^+\text{-}O)$ model is critical for quantitatively understanding the ionosphere.

Currently, there are three types of models for $\nu(O^+\text{-}O)$ in the ionosphere, as summarized in Figure 1 and Table 1. They are (1) the classic high-energy theory type (e.g., Banks, 1966; Schunk & Nagy, 2009), (2) the later wide-energy theory type (e.g., Stallcop et al., 1991, hereinafter S1991), and (3) the correction-factor type (e.g., Salah, 1993). There has been no laboratory experiment of the O^+-O collision at ionospheric thermal energies (~0.1 eV), but at superthermal energies (Stebbings et al., 1964, hereinafter S1964). Laboratory experiments have been used to justify theoretical $\nu(O^+\text{-}O)$ models, but have not been directly used to construct a $\nu(O^+\text{-}O)$ model. The present study constructs a laboratory-based model for the first time (see Section 4.2).

Collision frequency can be directly calculated from the collision cross section. The classic high-energy theory type model is based on the theoretical calculation of cross sections at energies above 1 eV. The resultant cross section is then extrapolated down to ionospheric energies. This classic model was constructed by Knof et al. (1964, hereinafter K1964) and has been adopted to formulate widely known sets of models (e.g., Banks, 1966; Schunk & Nagy, 2009), which include models of collision frequencies of other particle

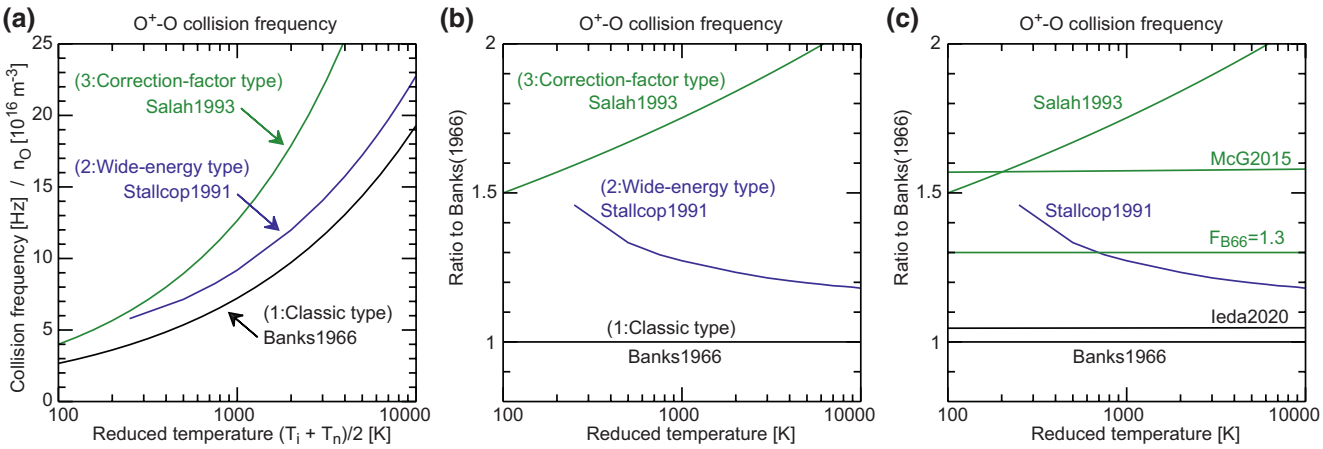

Figure 1. (a) Existing models of O^+-O momentum-transfer collision frequency. They are for the unit number density of atomic oxygen and are a function of the ion-neutral reduced temperature $(T_i + T_n) / 2$. A representative model of each of the three types of models is shown: (1) classic high-energy theory type (Banks, 1966), (2) later wide-energy theory type (Stallcop et al., 1991), and (3) correction-factor type (Salah, 1993). (b) The ratio of (a) to the Banks model, known as the Burnside factor, for each of the representative models. (c) Burnside factors of three additional models. See Table 1 for additional explanations.

pairs. This classic model has been widely used in ionospheric studies (e.g., Adachi et al., 2017; Brekke & Hall, 1988; Fang et al., 2013; Ieda et al., 2014; Kiene et al., 2019; Lomidze et al., 2015; Takeda, 2016), in particular, to calculate electric conductivity.

In contrast, the later wide-energy theory type model directly calculates the cross section at the ionospheric energy range. This later model was constructed by S1991 and was refined by Pesnell et al. (1993) and Hickman et al. (1997a). The present study does not focus on the differences between these later models, which are numerically small at ionospheric temperatures (6% at 1000 K). The later model has been compared with ionospheric observations (e.g., Anderson et al., 2013; Joshi et al., 2018; Nicolls et al., 2006) but has not been adopted for applications such as constructing conductivity models or running ionospheric simulations.

The classic collision frequency has been reported to be underestimated when compared to collision frequencies inferred from ionospheric observations (e.g., Burnside et al., 1987). The ratio of the inferred collision frequencies to the classic $\nu(O^+\text{-}O)$ model is called the Burnside factor. Salah (1993) multiplied the classic model by the Burnside factor to construct the correction-factor type model. This type of model has been widely used for ionospheric studies (e.g., Fang et al., 2013; McDonald et al., 2013; McGranaghan et al., 2015; Zossi et al., 2019), in particular, to run ionospheric simulations.

The Banks (1966) model has often been used as the basis model of the correction-factor model (e.g., Nicolls et al., 2006; Oliver & Glotfelty, 1996). In this study, we follow this tradition for calculations of the Burnside factor (F_{B66}) and the percentages. F_{B66} of various models is summarized in Table 1. For clarification, other classic models have been used as the basis model in some previous studies. Their temperature dependence is slightly different from the Banks (1966) model. Accordingly, F_{B66} of the Salah (1993) model is not constant in Figure 1b although it is recognized by them to be nearly constant between 700 and 1500 K. In such cases, we refer to F_{B66} at 1000 K. The Salah (1993) model corresponds to $F_{B66} = 1.752$ at 1000 K.

F_{B66} has been deduced using observed ionospheric parameters and momentum or energy equations. Estimated F_{B66} ranges from 0.7 to 1.9 (e.g., Dyson et al., 1997; Vickers et al., 2013; Wu et al., 2012) to date. This large variation is presumably due to various assumptions in the equations (e.g., Dang et al., 2015; Nicolls et al., 2006).

In particular, the neutral atomic oxygen density is not measured simultaneously with other ionospheric parameters but is assumed empirically. Note that a collision frequency model in the present study refers to a model of the collision frequency coefficient. This coefficient model is multiplied by the neutral density to obtain the collision frequency. Thus, the Burnside correction may not be relevant to the collision frequency coefficient model itself but to the assumed atomic oxygen density instead (e.g., Joshi et al., 2018).

Table 1
Models of O^+-O Momentum-Transfer Collision Frequency

Model type; Method; Original work	Ratio to Banks (1966) at 1000 K
(1) Classic high-energy theory type Theoretical calculation at superthermal energies and extrapolation down to ionospheric thermal energies; Knof et al. (1964) ("K1964") at 1–10,000 eV	1: Banks (1966) 1.046: Banks and Kockarts (1973) 1.049: Schunk and Nagy (2009) 1.047: Ieda (2020)
(2) Later wide-energy theory type Theoretical calculation directly including ionospheric thermal energies; Stallcop et al. (1991) ("S1991") at 0.027–52 eV	1.28: Stallcop et al. (1991) 1.31: Pesnell et al. (1993) 1.25: Hickman et al. (1997a)
(3) Correction-factor type A constant is multiplied to the classic model to be consistent with various ionospheric observations; Salah (1993) based on the classic model	1.75: Salah (1993) 1.26: Nicolls et al. (2006) 1.57: McGranaghan et al. (2015) 1.27: Joshi et al. (2018)
(4) Laboratory-experiment type Ion beam experiments at superthermal energies and extrapolation down to ionospheric thermal energies; Present study based on Stebbings et al. (1964) ("S1964") at 40–10,000 eV	1.22: "Unconverted" (present study) 1.15: "Converted" (present study) 1.23: "Ground-state" (present study)

Note. Some models are shown in Figure 1. Models represent collision frequency for the unit number density of atomic oxygen and are a function of temperature. The collision frequency ratio to a reference model is called the Burnside factor. The Burnside factors to the Banks (1966) model (F_{B66}) at 1000 K are shown. The laboratory-experiment type models are created in the present study in Section 4.2. The "ground-state" model is appropriate for ionospheric study. The definition of energy differs between laboratory experiments and theoretical studies (see Appendix A).

Nevertheless, appropriate statistical ionospheric observations have the potential capability to calibrate theoretical collision frequency (coefficient) models because the deviations of the simultaneous neutral atomic oxygen density from empirical models are expected to be averaged out. Later statistical observations tend to report $F_{B66} \sim 1.3$ (e.g., Joshi et al., 2018; Nicolls et al., 2006). Although this number has not yet been fully accepted, it is close to the later wide-energy theoretical model, labeled "Stallcop1991" in Figure 1c.

Thus, the later model could replace the classic model based on current ionospheric observation. However, the classic models are still widely used and have also been adopted as the basis of the correction-factor models. It is unclear why the later wide-energy model is not adopted for ionospheric applications.

We had hesitated to employ the later model because the following points had been unclear; thus, it appeared that the later model might include pitfalls. (1) In particular, both classic and later models are claimed to be consistent (within 6%) with the S1964 laboratory experiment; however, these consistencies appear to contradict the significant (30%) difference between the classic and later models. (2) It is also not clear whether the curved trajectory effect (Pesnell et al., 1994; Salah, 1993; Stubbe, 1968) is the primary cause of the difference between the classic and the later models. (3) Furthermore, the reference laboratory experiment (S1964) is contaminated by excited-state O^+ ions. Although the impact of this contamination on S1964 had been unknown, Salah (1993) supposed that this contamination caused the lesser cross section in the classic model. (4) Finally, the theoretical association between the classic and the later models is unclear because S1991 did not refer to K1964. A new model is not necessarily better than an old model.

The purpose of the present study is to confirm that the classic high-energy type O^+-O collision frequency model should be replaced by the later wide-energy-type model. We review the construction and verification of the classic model in Section 3. We then revise interpretations of the laboratory experiment that is used to justify theoretical models in Section 4. We clarify theoretical differences between the classic and later

Table 2
Definitions of Physical Parameters in This Study

Physical parameters	Definition
e	Fundamental charge, $1.602176634 \times 10^{-19}$ C
k_B	Boltzmann constant, 1.380649×10^{-23} J/K
g (m/s)	Relative velocity of an ion with respect to a neutral particle
m_i, m_n (kg)	Mass (ion, neutral particle)
μ_{in} (kg)	Reduced mass $m_i m_n/(m_i + m_n)$
ε_i (eV)	Ion kinetic energy $m_i v_i^2/2e$, where v_i is the ion velocity in the laboratory frame
ε_r (eV)	Reduced energy $\mu_{in} g^2/2e$ (also known as the kinetic energy of relative motion, see Table A1)
T_i, T_n (K)	Temperature (ion, neutral gas)
T_r (K)	Reduced temperature $(m_n T_i + m_i T_n)/(m_i + m_n)$
$q_D(\varepsilon_r)$, $q_E(\varepsilon_r)$ (m^2)	Energy-dependent cross section (diffusion, charge-exchange)
$\overline{Q}_D(T_r)$, $\overline{Q}_E(T_r)$ (m^2)	Temperature-dependent or average cross section (diffusion, charge-exchange)
ν (1/s)	Momentum-transfer collision frequency in the laboratory frame
n_n (1/m^3)	Number density of neutral gas
ν/n_n (m^3/s)	Collision frequency coefficient

Note. "Ion-neutral collision frequency" in the present study refers to the momentum-transfer collision frequency for momentum transfer from neutral gas in the laboratory frame.

models in Section 5. Implications of the correction-factor model are considered in Section 6. In Section 7, we discuss why the later model has still not been adopted.

2. Definitions and Basics

2.1. Definitions of Physical Parameters

The physical parameters used in this study are defined in Table 2. We use subscript D for the diffusion or momentum-transfer cross sections and subscript E for the charge-exchange cross sections.

2.2. Polarization Collision and Charge-Exchange Collision

There are two types of collisions between an ion and its parent neutral particle, such as between an O^+ and an O; these are scattering electric-polarization collision and resonant charge-exchange collision (e.g., Banks & Kockarts, 1973). The polarization collision is caused by the long-range attractive force that is due to the polarization of the neutral particle by the approaching ion. The charge-exchange collision is caused by the transfer of an electron from a neutral particle to an ion. The polarization collision dominates at low temperatures (i.e., low particle speeds and, thus, low kinetic energy), and the charge-exchange collision is dominant at high temperatures.

For the O^+-O collision, the transition temperature of the two collision domains has been thought to be approximately 230 K (Banks & Kockarts, 1973; Ieda, 2020; Schunk & Nagy, 2009), corresponding to 109 km altitude (COESA, 1976). Below this altitude (i.e., in the polarization domain), the O^+-O collision is usually not considered as important for ionospheric physics as the collision of other particle pairs such as NO^+-N_2. Accordingly, only the charge-exchange collision frequency is traditionally considered for the O^+-O collision.

2.3. Basics of Construction of Collision Frequency Model

A collision frequency model refers to a model of the collision frequency coefficient, which is the collision frequency divided by the number density of neutral gas. The collision frequency (coefficient) model for the ionosphere is traditionally expressed as a function of the reduced temperature, which is the mass-weighted average of ion and neutral temperatures. At a given temperature, particles with various kinetic energies contribute to the collision frequency. Accordingly, the energy-dependent diffusion cross section $q_D(\varepsilon_r)$ is the main body of a model. Once $q_D(\varepsilon_r)$ is obtained from theoretical or laboratory results, the collision frequency coefficient is calculated as follows.

$q_D(\varepsilon_r)$ is integrated over energy for each temperature to obtain the average cross section $\bar{Q}_D(T_r)$ as

$$\bar{Q}_D(T_r) = \frac{1}{2}\int_0^\infty q_D x^2 \exp(-x)dx, \tag{1}$$

where x is defined by $\varepsilon_r = xk_BT_r/e$. See Table 2 for the definitions of the physical parameters. This equation is equivalent to Equation 3 of Dalgarno et al. (1958) and Equation 7 of Hickman et al. (1997a). Numerical integration is necessary for general cases.

$\bar{Q}_D(T_r)$ is associated with the momentum-transfer collision frequency coefficient as

$$\nu_{LAB} / n_n = \frac{m_n}{m_i + m_n}\frac{4}{3}\sqrt{\frac{8k_B}{\pi\mu_{in}}}\sqrt{T_r}\bar{Q}_D, \tag{2}$$

in the laboratory frame. This equation is equivalent to Equation 9.78 of Banks and Kockarts (1973) and Equation 8 of Hickman et al. (1997a). This equation means that this collision frequency is defined as being independent of the relative bulk velocity between ion and neutral fluids, as is usual. This definition is reasonable for the charge-exchange collision when the relative bulk velocity is lower than the thermal velocity (Pesnell et al., 1994).

2.4. Approximation on Charge-Exchange Collision

The classic model neglects the long-range force in the resonant charge-exchange collision. Then, the resonant charge-exchange cross section $q_E(\varepsilon_r)$ can be given in the form of

$$q_E(\varepsilon_r) = (A_0 - B_0 \log_{10}\varepsilon_r)^2, \tag{3}$$

where A_0 and B_0 are constants that depend on the particle species. These constants are obtained from theoretical calculations or laboratory experiments. This approximate form was theoretically established by Dalgarno (1958b).

When $q_E(\varepsilon_r)$ is given by Equation 3, the integration (Equation 1) can be approximated using

$$\bar{Q}_E(T_r) = \left[(A_0 + R_T B_0) - B_0 \log_{10} T_r\right]^2, \tag{4}$$

where $R_T \sim 3.668$ and other constants are defined in Equation 3 (Banks, 1966; Ieda, 2020; Mason & Vanderslice, 1959; Pesnell et al., 1994). The neglect of the long-range force also implies an approximation:

$$\begin{cases} q_D(\varepsilon_r) = 2 \times q_E(\varepsilon_r) \\ \bar{Q}_D(T_r) = 2 \times \bar{Q}_E(T_r) \end{cases}. \tag{5}$$

The corresponding collision frequency can be obtained using Equation 2.

Note that this method is not used for the later wide-energy model because it includes the long-range force. Hence, Equation 3 does not strictly hold. Instead, numerical integration is used in Equation 1.

Table 3
O^+-O Energy-Dependent Charge-Exchange Cross Section

	Cross section (10^{-20} m^2)			
		Stebbings et al. (1964)		
Energy (eV)	(2) Knof et al. (1964)	(3) Unconverted	(4) Converted	(5) Ground-state
0.1	(36.8)	[43.3]	[40.8]	[43.9]
1	31.2	[35.4]	[33.2]	[35.6]
10	26.2	(28.3)	[26.3]	[28.3]
100	21.5	22.0	[20.3]	[21.8]
1,000	17.3	16.5	[15.0]	[16.1]
10,000	13.6	11.8	[10.5]	[11.3]

Note. The O^+-O charge-exchange cross sections q_E as a function of reduced energy, also shown in Figure 2. See detailed explanation in Figure 2 caption. The values shown in square brackets are calculated in this study. The other values are listed in Table 5 of Knof et al. (1964) ("K1964"), where the round parentheses indicate extrapolated values. K1964 compared their theoretical result in Column 2 with the Stebbings et al. (1964) laboratory result in Column 3. For clarification, we calculate the values 43.3 and 35.4 in Column 3 using Equation 37 in K1964, which is the same as Equation 7 of S1964. This equation is consistent with the other values in Column 3.

3. Original Construction and Justification of the Classic Model

3.1. Original Construction of Classic Model

The classic $\nu(O^+\text{-}O)$ model was originally constructed by K1964. There are many classic $\nu(O^+\text{-}O)$ models (e.g., K1964, Banks, 1966; Banks & Kockarts, 1973; Ieda, 2020; Schunk & Nagy, 2009; Schunk & Walker, 1973). They are based on $q_E(\varepsilon_r)$ of K1964 and are essentially the same, although they may appear slightly different because of different output styles, small errors, and numerical rounding. The classic model was recalculated from the K1964 cross section by Ieda (2020). This result is supposed to be accurate and is shown in Figure 1c by the line labeled "Ieda2020." The Banks (1966) model is an underestimation of this accurate model by 4% (Table 1), presumably due to a minor error (Ieda, 2020).

Before the classic model, Dalgarno (1958a) introduced the O^+-O charge-exchange collision concept for the diffusion of the F2 layer. However, Dalgarno (1964) noticed that the collision frequency of Dalgarno (1958a) was approximately three times that of the S1964 laboratory experiment. Accordingly, Dalgarno (1964) divided the Dalgarno (1958a) model by a factor of three to be close to the S1964 laboratory experiment. In other words, the Dalgarno (1964) model is conceptually similar to the correction-factor type model, where the Dalgarno (1958a) model is the basis.

K1964 improved the electric potential curve of the O^+-O system by including available spectroscopic data (see Section 5). K1964 calculated the $q_E(\varepsilon_r)$ above 1 eV and extrapolated the results down to ionospheric energies. This extrapolation is implicitly included in Equation 3. They insisted that their resultant $q_E(\varepsilon_r)$ is much closer to the S1964 laboratory ion beam measurement (5.5% difference) than the Dalgarno (1958a) model is.

Banks (1966) adopted the K1964 energy-dependent cross-section model from existing models because of this closeness. Banks (1966) stated, "according to Knof et al., the average deviation between the predicted and measured values is only 5.5 per cent. Therefore, the charge exchange cross section of Knof et al. will be used here." (p. 1115). That is, Banks (1966) does not appear to have confirmed this closeness. The Dalgarno (1964) model is consistent with the S1964 results by definition. However, Banks (1966) did not adopt the Dalgarno (1964) model, presumably because it includes a correction factor.

3.2. Original Justification of Classic Model

K1964 justified their results by insisting the closeness to laboratory measurements as follows. K1964 calculated the O^+-O $q_E(\varepsilon_r)$ at 1–10,000 eV and compared the results with the S1964 laboratory measurements at 40–10,000 eV in their Table 5. This comparison is shown in Columns 2 and 3 of Table 3. Figure 2a shows these values and Figure 2b shows their ratio. K1964 stated, "The average absolute deviation between the calculated and experimental values over the experimental energy range is only 5.5%." (p. 3553). Although we cannot determine how to reproduce this 5.5%, the deviation between the K1964 results in Column 2 of Table 3 and the S1964 results in Column 3 do appear small at superthermal energies; that is, 2% (21.5 to 22.0) at 100 eV.

However, we find that the slopes differ at ~100 eV, as shown in Figure 2b. As a consequence, the deviation is much larger at ionospheric energies, that is, 18% (36.8 to 43.3) at 0.1 eV. Thus, the K1964 results are not strongly supported by the laboratory measurements in the practical ionospheric context. Note that S1964 estimated ±25% uncertainty in the absolute magnitudes of the cross sections in their experiment. Accordingly, discussions of laboratory results are not definite within this order but focus on the most probable values for relative justification.

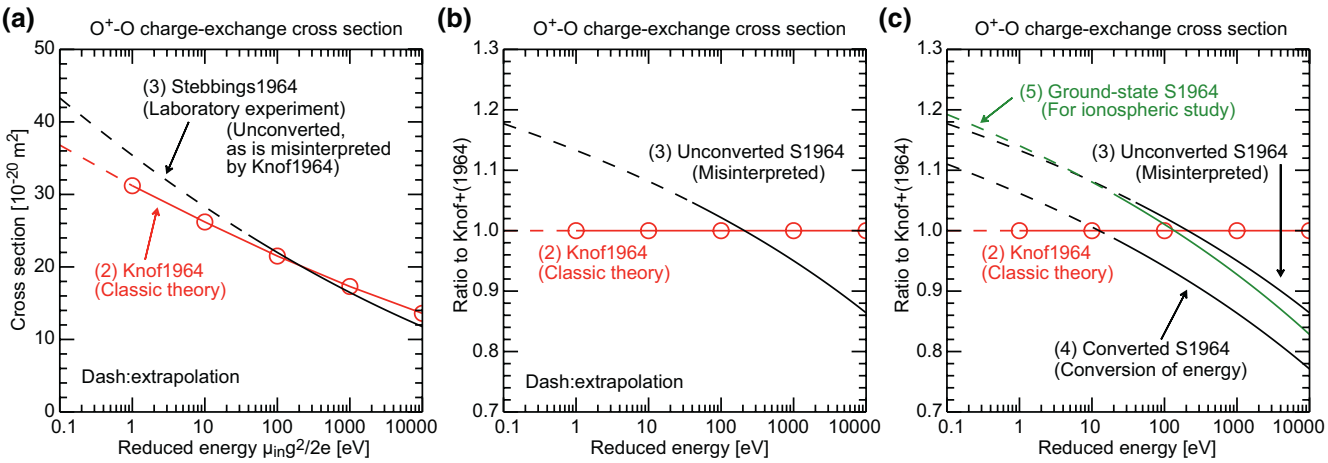

Figure 2. The O^+-O charge-exchange cross section q_E as a function of reduced energy, also shown in Table 3. The dashed lines indicate extrapolated energy ranges. (a) The Knof et al. (1964) ("K1964") theoretical result and the Stebbings et al. (1964) ("S1964") laboratory result. (b) The ratio of (a) to the K1964 values. (c) Similar to (b), but the S1964 results are shown in three formats: (3) "unconverted": as-is in K1964; that is, the energy of S1964 should be converted when referred in theoretical studies but is left unconverted in error; (4) "converted": energy of S1964 is converted correctly in the present study; (5) "ground-state": "converted" S1964 model is further adjusted to the ground-state O^+ case in the present study, assuming that measured O^+ is contaminated with the excited-state O^+ by 23%. This "ground-state" is our best interpretation of the laboratory results for ionospheric study and is higher than the K1964 result by 19% at 0.1 eV.

In summary, the classic $\nu(O^+\text{-}O)$ model was constructed theoretically by K1964. The K1964 model was adopted by the famous Banks (1966) model because K1964 insisted that their theoretical model was close to S1964 laboratory results. The S1964 laboratory measurement is not directly used to construct the classic $\nu(O^+\text{-}O)$ model; S1964 was used only for justification at superthermal energies.

4. Revised Interpretation of Laboratory Results

In this section, we correct and refine the original interpretation of the laboratory results made by K1964. As a result, we confirm that the classic model is not consistent with laboratory measurements, in contrast to the original interpretation by K1964.

4.1. Conventional Energy and Laboratory Contamination

Both classic and later theoretical models of O^+-O cross section $q_E(\varepsilon_r)$ justify themselves by consistency with the ion-beam laboratory experiment of S1964. However, there are two problems in the interpretation of the laboratory experiment. They are (A) conversion of energy and (B) contamination of excited-state O^+, as detailed respectively in Appendices A and B. The two problems are briefly explained in the following:

(A) *Conversion of energy*: The conventional definition of kinetic energy is two times different between theoretical studies and laboratory experiments. For example, 1 eV in theoretical studies corresponds to 2 eV in laboratory experiments. Thus, when the cross section is obtained by experiments, the corresponding energy should be divided by two in theoretical studies. However, K1964 shows the S1964 results without this conversion (Column 3 of Table 3). In contrast, we converted these "unconverted" $q_E(\varepsilon_{i,LAB})$ values in Column 3 to the "converted" $q_E(\varepsilon_r)$ values in Column 4 in Table 3. As a result, the "unconverted" values overestimate the "converted" values by approximately 9% at 100 eV (Figure 2c).

(B) *Contamination of excited-state O^+*: The S1964 laboratory measurements are contaminated by the excited-state O^+ ion, although the ground-state O^+ is relevant to the ionosphere. The impact of this contamination has been unknown and is not included in the classic model. We estimate that the original S1964 model has underestimated the cross section in the ionospheric context by 6.9%. Accordingly, we adjusted the "converted" values by multiplying it by 1/0.931~1.0741 to obtain the "ground-state" values

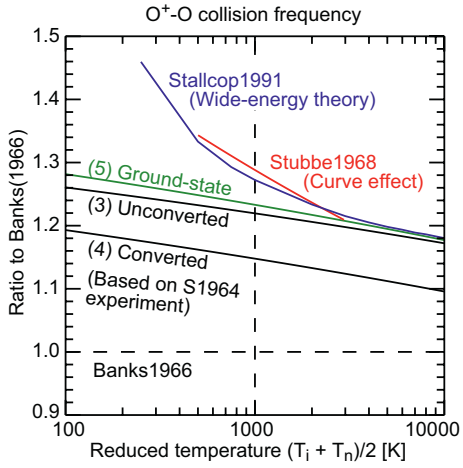

Figure 3. O^+-O momentum-transfer collision frequency models constructed in this study. They are a function of the ion-neutral reduced temperature and are shown as the ratio to the Banks (1966) model. Three versions of the models labeled (3), (4), and (5) are constructed based on a laboratory experiment by Stebbings et al. (1964). See detailed explanation in Figure 2 caption. The version labeled (5) "ground-state" is the best interpretation of the laboratory results for ionospheric study and is higher than the Banks (1966) result by 23% at 1000 K. The Stubbe (1968) and the Stallcop et al. (1991) models are also shown.

in Column 5 of Table 3. As a result, "ground-state" results are close to the "unconverted" results within approximately 1% between 0.1 and 100 eV, as shown in Figure 2c.

This indicates that the (A) conversions and (B) adjustments coincidentally cancel each other. Accordingly, the closeness in values and the differences in slopes at high energies between the K1964 and the S1964 results are not significantly altered by this revision. Note that the contamination effect is now included as a result of our revision.

4.2. Construction of a Laboratory-Based Collision Frequency Model

In this section, we construct collision frequency models based on laboratory experiments. "Unconverted," "converted," and "ground-state" versions of S1964 $q_E(\varepsilon_r)$ discussed in Section 4.1 are given by Equations A2, A3, and B3, respectively. Because these $q_E(\varepsilon_r)$ values are already expressed in the form of Equation 3, $\bar{Q}_D(T_r)$ can be obtained using Equations 4 and 5. Accordingly, the collision frequency can be obtained using Equation 2. For example, the resultant "ground-state" S1964 model is

$$\bar{Q}_E(T_r) = 1.0741 \times (8.0712 - 0.63 \times \log_{10} T_r)^2 \times 10^{-20}, \quad (6)$$

$$\nu_{LAB} / n_n = 34.297\sqrt{T_r}\, 2\bar{Q}_E = 0.4800\sqrt{T_r}\,(1 - 0.07806 \times \log_{10} T_r)^2 \times 10^{-16}. \quad (7)$$

Figure 3 shows the Burnside factor of these models. The "ground-state" model is our best interpretation of the S1964 laboratory measurement for ionospheric study. The value at 1000 K exceeds the value obtained from the Banks (1966) model by 23%.

4.3. Curved Particle Trajectory Effect

The laboratory-based models do not include the curved trajectory effect by definition. In this section, we discuss that the curved trajectory effect was overestimated (28% at 1000 K) by Stubbe (1968).

The long-range attractive polarization force makes particle trajectories curved, and thus increases the effective charge-exchange cross section. Accordingly, the actual O^+-O charge-exchange cross section is increasingly higher than Equation 3 as the temperature decreases. This effect is not included in the classic high-energy model. Knof et al. (1964) and Banks (1966) recognized that this effect was small; i.e., at most 11% at the transition temperature (235 K), implying that this effect is negligible at 1000 K.

In contrast, Stubbe (1968) insisted that the curved trajectory effect should be included; they estimated that the effect increased the collision frequency by 28% at 1000 K from the Banks (1966) model. This Stubbe (1968) result was mentioned by Salah (1993) and Pesnell et al. (1994) and is likely to be recognized as responsible for the 30% difference between the classic and later models.

However, Stubbe (1968) incorrectly assumed that Banks (1966) adopted the S1964 cross section. In reality, Banks adopted the K1964 cross section instead, as explained in Section 3. This misunderstanding is also pointed out by Carlson and Harper (1977). Accordingly, the contribution of the curved trajectory effect is not 28% (from "Banks1966" to "Stubbe1968" in Figure 3), but only 5.8% (from "Unconverted" S1964 to "Stubbe1968" in Figure 3) at 1000 K. For some clarification, Stubbe (1968) did not convert energy. We calculate that the ratio of the Stubbe (1968) model to the Banks (1966) model is 29%, not 28%.

Nevertheless, the slope of the Stubbe (1968) model appears close to the later wide-energy model (S1991) at approximately 1000 K in Figure 3. This closeness suggests that the Stubbe (1968) calculation of the curved

trajectory effect itself is correct and that this effect is consistent with the long-range force that is included in the later wide-energy model.

4.4. Summary of the Revised Interpretation

The result from the "ground-state" laboratory-based model ($F_{B66} = 1.23$ at 1000 K) is close to that from the S1991 model ($F_{B66} = 1.28$ at 1000 K), particularly when the curved trajectory effect (~6% at 1000 K) is added. Hence, the classic model ($F_{B66} \sim 1$) should be replaced by the later model, based on laboratory results.

The 28% difference in $\nu(O^+\text{-}O)$ at 1000 K between the Banks (1966) and S1991 models includes the core difference of 19% as well as the nonessential error of 4% in the Banks (1966) model (see Section 3.1). The remaining 5% is presumed to be due to the curved trajectory effect (~6%). The core difference corresponds to the difference of approximately 19% between the classic and the "ground-state" laboratory results at approximately 0.1 eV, as shown in Figure 2c. The core difference implies that the slope or energy dependence of the cross section is less accurate in the classic theory. Note that values are calculated or measured only at high energies in the classic high-energy model and in the laboratory experiment; values at low energies are obtained by extrapolating the slope.

5. Theoretical Differences

In this section, we clarify the theoretical differences between the classic high-energy model and the later wide-energy model. There are several updates from K1964 (the classic model) to S1991 (the later model), but it is often difficult to identify the impact of each update. We broadly discuss selected updates in this section. The key difference is in the potential curve as explained below.

5.1. Potential Curve

Collision frequency or cross-section models depend largely on the electric potential of the ion-neutral particle pair system. This potential is a function of the internuclear separation distance and is called the interaction potential curve. The classic models are based on the potential curve constructed by K1964 for the O^+-O system, whereas the later models are based on the potential curve constructed by S1991.

Dalgarno (1958a) speculated the potential curve by referring to the ionization potential of atomic oxygen. K1964 enhanced Dalgarno (1958a) by including spectroscopic data of dissociation energy for some electronic states to improve the potential curve. K1964 had been the best-known approach (Capitelli et al., 1977). However, K1964 is not cited by S1991, presumably because it was recognized as outdated.

The energy dependence of the charge-exchange cross section depends on the functional form of the potential curve. Stallcop (1971) pointed out that the functional form used for the potential curve in K1964 should be modified depending on spin multiplicity, as Capitelli et al. (1977) explain that Stallcop (1971) improved the K1964 approach, "by constraining the doublet molecular wavefunctions to transform properly also under inversion through the middle-point of the internuclear distance." (p. 269). That is, the energy dependence of K1964 at high energy was in error and was corrected by Stallcop (1971).

Capitelli et al. (1977) suggested that the N^+-N cross section of K1964 is underestimated by 30% without this correction. This is presumably associated with the fact that the energy dependence of the N^+-N cross section is less significant in K1964 than in Capitelli et al. (1977), as seen in Figure 3 of Capitelli et al. (1977). Thus, the O^+-O cross section would also be significantly affected.

Stallcop and Partridge (1985) do not refer to K1964, but updated Stallcop (1971) by including the outer boundary area of the charge exchange. This update appears to increase the N^+-N cross section by 5% in Figure 3 of Stallcop and Partridge (1985). Thus, it is likely that the O^+-O cross section was also affected by about 5%. S1991 also included several revisions to the potential curve without any explanation of the impacts, as outlined in Partridge and Stallcop (1986).

5.2. Mechanics and Long-Range Force

Differences between the mechanical methods for K1964 and S1991 are not likely to have a significant impact at high energies, as explained in the following paragraphs. Approximations in quantum mechanics may be introduced for atomic and molecular collisions because the de Broglie wavelength is relatively short. Both K1964 and S1991 invoke semiclassical approximations.

K1964 used the impact parameter method. This relatively simple method is valid only at high energies because it assumes straight particle trajectories. That is, the long-range polarization force and the resultant curved particle trajectory effect are not included. In addition, this method does not determine the rapid quantum oscillations of the electron transfer probability against the impact parameter that characterize close collisions. Instead, it invokes the random phase approximation, which means that the probability of electron transfer from a neutral particle to an ion in a close collision is taken to be 1/2.

S1991 used quantum mechanics with the semiclassical Wentzel-Kramers-Brillouin approximation; that is, only the first-order perturbation of the Planck constant is considered for the nuclear wave function in the O^+-O quasi-molecule. This method can include the long-range force, which, however, is negligible above 1 eV. It can also include some discrete structures such as orbiting and glory resonances. However, such structures are mostly averaged out when the cross section is integrated over energy (Heiche & Mason, 1970).

For clarification, Hickman et al. (1997a) used full quantum mechanics, although we classify it the same type as S1991 because the potential curve is mostly based on S1991. Quantum spin-orbit interaction effects are important below approximately 300 K, but average out at higher temperatures, where the particle kinetic energy is much larger than the spin-orbit splitting. Accordingly, the differences in method between Hickman et al. (1997a), K1964, and S1991 do not cause significant differences in cross sections at high energies (i.e., above 1 eV).

5.3. Summary of Theoretical Difference

We have discussed theoretical differences between K1964 and S1991 that potentially cause the difference in the cross section. Several improvements were introduced to K1964. Although we are unable to precisely estimate the impact of each factor, the major cause appears to be in the potential curve and not mechanics, presumably associated with the correction by Stallcop (1971). This error associated with spin multiplicity appears to cause an error in the energy dependence (slope) of the cross section of K1964.

Because many corrections were applied to the K1964 model, it is theoretically outdated. Thus, we hesitate to use the classic model that is based on K1964. The later model (e.g., S1991) is the corrected descendant of the classic model; they share the core idea, which is electronic structure calculations combined with available spectroscopic data to construct their potential curves. Thus, from the theoretical point of view, the classic model should be replaced by the later model. In addition, the later model includes the long-range force because the mechanics were also improved for describing lower energy.

6. Implications of Correction-Factor Model

The correction-factor type $\nu(O^+\text{-}O)$ model is a correction of the classic model with a constant factor (see Section 1). In this section, we consider the implications of this model.

6.1. Original Proposal

Salah (1993) proposed the correction-factor type model, motivated by ionospheric observations at that time ($F_{B66} \sim 1.75$). Salah (1993) claimed that "It is clear that the early values derived by Dalgarno (1964), Banks (1966), and Schunk and Walker (1973) are too low, since they are primarily based on laboratory measurements that require confirmation due to the effects of beam contamination. Theoretical formulations such as Stubbe (1968), Stallcop et al. (1991), and Pesnell et al. (1993) favor a 30% increase over the early models" (p. 1545). Salah (1993) also stated that "Unpublished theoretical calculations [A. Dalgarno, private

communication, 1992] result in a collision cross-sections that are a factor of 1.5 larger than the results by Stallcop et al." (p. 1544).

Thus, Salah (1993) believed that the classic model is based on laboratory results and is underestimated due to laboratory contamination. They presumably thought that laboratory contamination can be corrected by a constant. Accordingly, they selected the classic model as the basis to be corrected by a constant. Salah did not select the later theoretical model (e.g., S1991), presumably in anticipation that this model will be taken over by a future correct theoretical model (i.e., the private communication), which would be more consistent with ionospheric observations at that time.

For clarification, we state for simplicity that Salah (1993) adopted the classic model as the basis model. Strictly speaking, their basis model is neither the same as the Dalgarno (1964) nor the classic models but is a simplified version of these models. Salah (1993) recognized that these models (the Dalgarno, classic, and their models) were primarily based on laboratory measurements and were essentially the same in their context.

6.2. Misunderstanding in Original Proposal

However, it is a misunderstanding that the classic model is based on laboratory measurement. In reality, the classic model is based on the K1964 theoretical result (see Section 3). This misunderstanding could have been noticed if the classic model and the laboratory result were numerically compared (Figure 3). In other words, the laboratory result was not shown in Salah (1993) presumably because they misunderstood that the classic model was based on the laboratory result.

Due to this misunderstanding, the correction-factor model adopted the classic model as its basis, intending a calibration of laboratory contamination. In contrast, the classic model is based on theory, and thus laboratory contamination is irrelevant. Hence, the physical reasoning behind the correction-factor model does not make sense.

Salah (1993) also recognized that the result of the S1991 model was 30% higher than the laboratory expectation. This second misunderstanding presumably occurred due to their first misunderstanding. In reality, the S1991 model is close to laboratory expectation (within ~5% at 1000 K, Figure 3). Furthermore, there is no follow-up theoretical study to verify the private communication (see Section 6.1).

6.3. Current and Future Implications

The classic model is not based on a laboratory experiment. Thus, the original correction-factor type concept should be rejected. Although a constant correction factor to collision frequency may still be useful, a constant cannot correct the classic model, because the error of the classic model is temperature-dependent. Thus, the basis model should be the later wide-energy model. This model is already consistent with the contamination-adjusted laboratory model. Accordingly, the correction by a constant is neither for the contamination nor the later wide-energy collision frequency (coefficient) model itself, but for the neutral atomic oxygen density.

7. Discussion

7.1. Primary Concerns in This Study

As introduced in Section 1, we had hesitated to employ the later wide-energy model because we were concerned that the following four points were unclear. We have clarified them in support of this model as follows:

(1) The classic and the later models are different by 30% at 1000 K even though both models had been claimed to be consistent with laboratory experiments. We clarified this discrepancy in Sections 3 and 4. That is, the later model is consistent with the laboratory-based model, but the classic model is consistent only at superthermal energies (~100 eV).

(2) The S1964 laboratory experiment was contaminated by excited-state O^+. We estimated that the impact of this contamination on the measured cross section was small (7.4%). Meanwhile, we noticed that conventional laboratory energy was misinterpreted in previous theoretical studies, causing a conversion error. We estimated that the contamination and this misinterpretation coincidentally tend to cancel each other (see Section 4.1).
(3) The curved particle trajectory effect had been estimated to be 28% at 1000 K (Stubbe, 1968). We clarified that the curved trajectory effect contributes only 6% at 1000 K to the cross section (see Section 4.3).
(4) Theoretical association between the classic and the later models was not readily clear because K1964 is not referenced by S1991. We now recognize that the S1991 model is the correction and update of K1964 (see Section 5).

7.2. Why Has the Later Model Still Not Been Adopted?

As explained in Section 1, it is known that the later wide-energy model is closer to current statistical ionospheric observations ($F_{B66} \sim 1.3$) than the classic high-energy model is. Thus, the classic model should have been replaced by the later model from the ionospheric observation point of view. In this section, we discuss why the later model has still not been adopted.

A possible reason may be tradition. The later model has not been adopted by previous studies, in particular, by Salah (1993). The later model is not widely known because it is not mentioned in key textbooks (i.e., Brekke, 2013; Kelley, 2009; Schunk & Nagy, 2009).

The core reason is presumably that the classic model (e.g., Banks, 1966; Schunk & Nagy, 2009) is misunderstood as based on laboratory experiments. Namely, it is often misunderstood (e.g., Buonsanto et al., 1997; Lindsay et al., 2001; Pesnell et al., 1993; Salah, 1993; Stubbe, 1968) to be the case that the classic model is based on the S1964 laboratory result. In reality, the classic model is based on the K1964 theoretical model. This misunderstanding could have been noticed if the classic model and the laboratory result had been numerically compared (Figure 3). In other words, this misunderstanding is likely why there has been no explicit collision frequency model that is based on laboratory measurement.

The cause of this misunderstanding may be a coincidence as follows. Dalgarno (1964) thought that the collision frequency of the Dalgarno (1958a) theoretical model was approximately three times higher than the S1964 laboratory experiment, and divided the Dalgarno (1958a) model by a factor of three (see Section 3.1). The resultant Dalgarno (1964) model ($F_{B66} = 1.01$ at 1000 K) is similar to the Banks (1966) model ($F_{B66} = 1$).

This similarity (1%) may give the impression that the Banks (1966) model should also be extremely close to laboratory results. Furthermore, the extreme closeness may appear to support the recognition that the classic model is based on the laboratory result. Note, however, that Dalgarno (1964) presumably intended a rough calibration, using the factor of three. The resultant Dalgarno (1964) model is not so close to the laboratory results (e.g., 14%–22% at 1000 K, as shown in Table 1).

In some other previous studies, the classic model was recognized as a theoretical model, but was often interpreted as being in "reasonable agreement" with laboratory results (e.g., Burnside et al., 1987; Nicolls et al., 2006). This lack of clarity was partly inevitable because the impact of laboratory contamination was unclear.

In summary, the Dalgarno (1964) model is extremely close to the Banks (1966) model by a rare coincidence. This coincidence presumably endorsed the misunderstanding that the classic model is based on laboratory results. The classic model was adopted as the basis due to this misunderstanding, and is still used presumably by tradition. As a consequence, the superior merit of the latter model has not been appreciated.

7.3. Slope of Lindsay Laboratory Results

Lindsay et al. (2001) performed the most recently reported laboratory measurement of the O^+-O collision cross section. They insist that their results are consistent with the Salah (1993) model ($F_{B66} \sim 1.75$). This conclusion prevents definitive consensus on the Burnside problem (e.g., Nicolls et al., 2006) and thus is

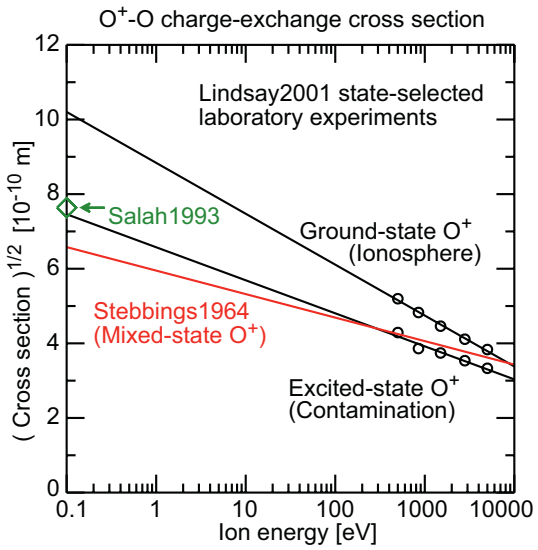

Figure 4. The O^+-O charge-exchange cross section q_E against ion kinetic energy in the laboratory frame ε_i. Laboratory measurements by Stebbings et al. (1964) (red) at 40–10,000 eV and Lindsay et al. (2001) (black) are compared. Circles indicate the Lindsay et al. (2001) measurements at five ion energies (500, 850, 1500, 2800, and 5000 eV). Corresponding least-square regression lines are calculated in the present study: $q_E^{1/2} \times 10^{10} = 8.838 - 1.364 \times \log_{10}\varepsilon_i$, correlation coefficient cc = −0.997 for the ground-state; $q_E^{1/2} \times 10^{10} = 6.576 - 0.8852 \times \log_{10}\varepsilon_i$, cc = −0.974 for the excited-state. The green diamond shows the Salah (1993) model $q_E = 58.3 \times 10^{-20}$ m^2, which is independent of energy.

likely another reason why the later model ($F_{B66} \sim 1.3$) is not adopted in ionospheric applications. We clarify this conclusion as follows.

S1964 measured the cross section at 40–10,000 eV, where O^+-states are mixed. Lindsay et al. (2001) measured the cross section at 500–5,000 eV, where O^+-states are separated. They identified that the S1964 result with mixed-state O^+ lies between their ground- and excited-state results (Figure 4) and, in this regard, insisted that their experiment is consistent with the S1964 results.

Confusingly, Lindsay et al. (2001) also concluded that their results are consistent with Salah (1993). Lindsay et al. (2001) did not show a line that represents an extrapolation of their results in Figure 4 of their paper but pointed to the cross section that is 1.7 times greater than that of S1964. This factor of 1.7 implicitly invokes the Salah (1993) model. As a result, their conclusion may tend to be interpreted that an extrapolation of the Lindsay et al. (2001) ground-state results is consistent with Salah (1993).

However, this interpretation is incorrect, as shown in Figure 4. An extrapolation of the Lindsay et al. (2001) ground-state results corresponds to $q_E = 104 \times 10^{-20}$ m^2 and $F_{B66} = 2.8$ at 0.1 eV, which is much larger than the Salah (1993) model ($F_{B66} \sim 1.75$). For clarification, Lindsay et al. (2001) misunderstood that the classic model is based on laboratory results and thus overestimated the Salah (1993) model.

The unrealistically high cross section ($F_{B66} = 2.8$ at 0.1 eV) stems from the steep slope. The slope or energy dependence of the cross section is steeper in their ground-state results than in the S1964 results (Figure 4). However, Lindsay et al. (2001) did not discuss the difference in slope. Instead, Lindsay et al. (2001) prohibited extrapolation of their results down to ∼ 0.1 eV, stating that "The present results for ground state ions cannot be used to estimate the thermal energy cross section with any degree of accuracy because of their limited energy range and the associated uncertainties." (p. 8202). Thus, neither an extrapolation nor the slope is relevant to their conclusion.

Instead, the reason of their conclusion is that "the charge transfer cross section for ground state ions is larger than that for excited ions and may thus be considered as lending support to a larger value for the thermal energy cross section than was inferred from the earlier laboratory work" (p. 8202). That is, they intended to state that a correct model should be higher than the S1964 result because of the contamination.

However, the impact of contamination is only 7%, as estimated in Section 4.1. Thus, the S1964 model is valid, especially after the small adjustment for this impact. For clarification, the contamination is independent of ion energy, as Lindsay and Stebbings (2005) do not mention a dependence on ion energy when they discuss the contamination.

In summary, Lindsay et al. (2001) concluded that their result of O^+-O cross section is consistent with the Salah (1993) model. Note however that Lindsay et al. (2001) prohibited extrapolations of their results. Thus, they do not intend to exclusively support the Salah (1993) model in their logical flow. The adjusted S1964 model is consistent with the later model, which means that the result of Lindsay et al. (2001) is more consistent with the later model than with the Salah (1993) model.

8. Conclusion

This study compared the various O^+-O collision frequency coefficient models. Currently, the classic theoretical model (e.g., Banks, 1966; Schunk & Nagy, 2009) is widely used, often with a correction factor. In contrast, the later theoretical model (e.g., Stallcop et al., 1991) is not used for ionospheric applications. We conclude that the classic model should be replaced by the later model, primarily because the later model is the theoretical correction and improvement of the classic model.

It has often been misunderstood that the classic model is based on laboratory results. Owing to this misunderstanding, the correction-factor model (e.g., Salah, 1993) has adopted the classic model as its basis, intending a calibration of laboratory contamination. In reality, the classic model is based on Knof et al. (1964) theory. Thus, the original purpose of the correction-factor model does not make sense. The energy-dependent error in the classic model cannot be corrected by a temperature-independent constant.

A correction factor to collision frequency may be useful if its basis is the later theoretical model. In this case, the constant essentially implies a correction of assumed neutral atomic oxygen density. Simultaneous observation of atomic oxygen is necessary for further evaluation of the collision frequency coefficient model. The later model may not be final but is better than the classic model from all points of view (ionospheric observation, laboratory experiment, and theoretical study).

Appendix A: Conventional Energy in Laboratory Experiment and Theory

We detail the conversion of kinetic energy that is mentioned in Section 4.1. Kinetic energy is not defined with an equation in previous studies. Accordingly, it may not be remembered that the conventional definition of kinetic energy is different across laboratory experiments and theoretical studies. For the collision of a parental particle pair such as O^+-O, the conventional energy in a laboratory ion beam experiment is twice that in a theoretical study (Appendix A1). This relationship should have been used in previous studies (Appendix A2). However, the energy used in the S1964 laboratory experiment was not converted in K1964 and S1991 theoretical studies. As a result, the energy-dependent cross section of the laboratory results is overestimated in these theoretical studies by approximately 9% at 100 eV (Appendix A3).

A1 Summary of Conventional Kinetic Energy

The conventional definitions of kinetic energy are summarized in Table A1. For simplicity, the parameters in the theoretical study are approximated for collisions between parental particle pairs such as O^+-O. That is, the ion mass m_i and the neutral mass m_n are practically the same. We consider the same collision with relative velocity g from two different points of view (i.e., laboratory experiment and theoretical study).

Table A1
Conventional Definition of Kinetic Energy for Parental Ion-Neutral Collision

	Laboratory experiment	Theoretical study
Frame	Laboratory	Center-of-mass
Relative velocity (m/s)	g	g
Ion velocity v_i (m/s)	g	$\sim g/2$
Neutral velocity v_n (m/s)	0	$\sim -g/2$
Reduced mass (kg)		$\mu_{in} \equiv m_i m_n/(m_i + m_n) \sim m_i/2$
Conventional energy (eV)	$\varepsilon_{i,LAB} \equiv m_i v_i^2/2e = m_i g^2/2e \sim 2\varepsilon_r$	$\varepsilon_r \equiv \mu_{in} g^2/2e \sim (m_i/2) g^2/2e = m_i g^2/4e \sim \varepsilon_{i,LAB}/2$
Term for energy	Ion energy[a]	Reduced energy[b]

Note. The conventional definition of energy for the ion-neutral collision is different across laboratory ion beam experiments and theoretical studies. These definitions were not shown with equations in previous studies and they are inferred by the present study. This table is valid only when ion and neutral masses are practically the same, that is, for the collision of a parental particle pair such as O^+-O.

[a]Also termed: ion energy (Stebbings et al., 1964); energy of the incoming ion (Rutherford & Vroom, 1974); and projectile energy (Lindsay et al., 2001; Lindsay & Stebbings, 2005). [b]Also termed: energy (Knof et al., 1964); kinetic energy of relative motion (Banks, 1966; Pesnell et al., 1994); collision energy (Stallcop et al., 1991); kinetic energy of the reduced mass particle (Pesnell et al., 1993); and kinetic energy (Hickman et al., 1997a).

Table A2
Correspondence of Conventional Kinetic Energies

(a) Ion energy in laboratory, $\varepsilon_{i,LAB}$ (eV)	(b) Reduced energy, ε_r (eV)	(c) Reduced temperature, T_{kT} (K)	(d) Reduced energy, ε_r (a.u.)
$\sim 2\varepsilon_r$ (eV)	$\sim \varepsilon_{i,LAB}$ (eV)/2	$\sim$11,604.52 ε_r (eV)	$\sim \varepsilon_r$ (eV)/27.21139
54.423	27.211	315,775	1
4	2	23,209	0.073499
2	1	11,605	0.036749
1	1/2	5,802	0.018375
0.34469	0.17235	2,000	0.0063336
0.17235	0.086173	1,000	0.0031668

Note. Example correspondence of conventional kinetic energies for parental ion-neutral collision. See Table A1 for definitions. A collision between a parental particle pair such as O^+ and O is supposed; that is, the ion mass and the neutral particle mass are assumed to be the same. (a) Conventional energy in laboratory ion beam experiment. (b) Corresponding conventional energy in theoretical study. (c) The reduced temperature defined by $T = e\varepsilon_r/k_B$. Note that other definitions are possible. (d) Similar to (b), but in the atomic unit in the Hartree definition.

In this study, the laboratory experiment refers to the ion beam experiment by S1964. Ion beam experiments eject the O^+ ion at velocity $v_i = g$, which will collide the target neutral atomic O that presumably has initial velocity $v_n = 0$ in the laboratory frame. The relative velocity $g = v_i - v_n$ is independent of the frame. As a result, conventional energy in the laboratory experiment is twice that in the theoretical study (Table A1). Corresponding examples of numerical values are listed in Table A2.

A2 Indirect Evidence for the Existence of Different Conventional Definitions

In this section, we evaluate the conventional definitions of kinetic energy (Table A1) used in previous studies. Energy is generally not explicitly defined with an equation in previous studies, presumably because the definition of energy is evident within each scientific community. In other words, the same definition is likely used within each scientific community if there is no explicit explanation. The frame is also generally not explicitly defined in previous studies. In such studies, the frame is presumably the laboratory frame for laboratory experiments and the center-of-mass frame for theoretical studies.

We first confirm indirectly that "ion energy" in the S1964 laboratory experiment conventionally refers to $\varepsilon_i = m_i v_i^2/2e$ that is defined in the laboratory frame. This interpretation is numerically consistent with the relationship for O^+ between ion energy of 1 eV and ion velocity of 3.5×10^3 m/s shown in Table 4 and Figure 7 of Stebbings et al. (1966). Thus, our interpretation is presumably correct also in S1964.

In contrast, we interpret that "energy" in the K1964 theoretical study conventionally refers to $\varepsilon_r = \mu_{in} g^2/2e$. We call this energy "reduced energy" associated with reduced mass to avoid confusion. This equation is not explicitly shown in previous theoretical studies (e.g., Banks, 1966; Hickman et al., 1997a, 1997b; K1964; Pesnell et al., 1993; Pesnell et al., 1994; S1991). However, our interpretation is consistent with the term "the kinetic energy of the reduced mass particle" in Pesnell et al. (1993). Additional indirect evidence for this interpretation is that our reduced energy is equivalent to energies used in equations in some other theoretical studies, including "the energy of relative motion of an ion and a gas particle" in Equation 4 of Dalgarno et al. (1958) and "the relative energy of collision" in Equation 16 of Heiche and Mason (1970).

In summary, we have indirectly confirmed that the conventional energies are used in previous studies for O^+-O collision. Thus, the energy used in laboratory experiments should be converted by previous theoretical studies (Table A1).

A3 Conversion of Energy-Dependent Cross Section from Laboratory Experiment to Theory

According to the discussion in Section A2, the S1964 laboratory experiment presumably used the ion energy in the laboratory frame. Similarly, the K1964 theoretical study presumably used the reduced energy to show their results. Thus, K1964 should have converted the S1964 results in their Table 5 (our Table 3). However, K1964 showed q_E in their Equation 37 as is originally given in Equation 7 of S1964 as

$$q_{E,S1964}^{Unconverted} = (5.95 - 0.63 \times \log_{10} \varepsilon_{i,LAB})^2 \times 10^{-20}. \quad \text{(A1)}$$

K1964 should have converted this equation using $\varepsilon_{i,LAB} = 2\varepsilon_r$ to

$$q_{E,S1964}^{Converted} = (5.95 - 0.63 \times \log_{10} 2\varepsilon_r)^2 \times 10^{-20} = (5.7604 - 0.63 \times \log_{10} \varepsilon_r)^2 \times 10^{-20} \quad \text{(A2)}$$

For example, the cross section (in 10^{-20} m^2) of Equation A1 is 21.996 at 100 eV and 20.253 at 200 eV, and their ratio is 1.09. These values are valid when energy refers to the ion energy in the laboratory experiment convention. However, K1964 presumably intended to show the S1964 results against the reduced energy. That is, the value of q_E at 200 eV in Equation A1 should have been used as the value at 100 eV in K1964. The lack of this conversion results in a 9% overestimation (i.e., 20.253 to 21.996) at 100 eV of reduced energy. That is, the value of 22.0 in Table 5 of K1964 (Column 3 of our Table 3) should have been 20.3, as shown in Column 4 of our Table 3, for example. Similar calculations show overestimations of 10% at 1 keV and 6% at 0.1 eV.

Similarly, S1991 should have divided the S1964 energies by two. For example, the value of the cross section in S1964 originally at 40 eV (i.e., ion energy in the laboratory convention) should have been plotted at 20 eV (i.e., reduced energy) in Figure 5 of S1991. However, the 40 eV (lowest energy) data point of S1964 is shown approximately at 40 eV (i.e., $40/27.21 \sim 10^{0.17}$ a.u.) in Figure 5 of S1991. It should have been at 20 eV (i.e., $20/27.21 \sim 10^{-0.13}$ a.u.). Thus, S1991 did not convert the energy in error, as well.

For clarification, the unit of energy is "atomic units" in Figure 5 of S1991 without further explanation. We notice that the unit of energy is "Eh" in Stallcop et al. (1998). Thus, we assume that the Hartree definition (not Rydberg definition) was used in S1991. Accordingly, 1 a.u. corresponds to 27.21139 eV.

Another clarification is that Table 4 of Banks (1966) refers to the S1964 laboratory result as the coefficients of $A_0 = 5.88$ and $B_0 = 0.57$ in 10^{-10} m (see our Equation 3). These coefficients are somewhat different from those in Equations A1 and A2 and thus are probably typographical errors. However, these errors do not affect the Banks (1966) model because their model is not based on the S1964 result.

Appendix B: Excited-State O^+ Contamination in Laboratory Experiments

The O^+-O collision in the ionosphere practically occurs between the ground-state O^+ and ground-state O. However, the S1964 laboratory experiment is contaminated with excited-state O^+. Accordingly, we adjust the cross section of S1964 by multiplying it by a factor of 1.0741 for ionospheric study in Section 4.1. In this section, we describe our estimation of this factor.

B1 Impact of Contamination

Lindsay et al. (2001) measured the ground-state cross section $q_{E,ground}$ in a limited energy range (500–5,000 eV) using a filtering technique. They also measured the mixed-state (ground- and excited-state) cross section $q_{E,mixed}$. The excited-state cross section $q_{E,excited}$ was not measured but calculated presumably using an association of sum:

$$q_E^{mixed} = f_{e/m} q_E^{excited} + \left(1 - f_{e/m}\right) q_E^{ground}, \tag{B1}$$

where $f_{e/m}$ is the fraction of number density (excited-state to mixed-state O^+), which was measured but not reported. As a result, they estimated that $q_{E,excited} \sim 0.7 \times q_{E,ground}$.

This result is supposed to be independent of the details of each experiment. Thus, substituting into Equation B1 yields

$$q_E^{mixed} / q_E^{ground} = 1 - 0.3 f_{e/m}. \tag{B2}$$

The fraction $f_{e/m}$ depends on the details of each experiment and is not measured by S1964. We assume $f_{e/m} = 0.23$, as it will be discussed in section B2. Then, we find that the S1964 O^+-O cross section is underestimated by 6.9% for ionospheric purposes. Accordingly, we multiply Equation A2 by a factor of $1/0.931 \sim 1.0741$ to deduce the ground-state O^+ cross section (see Section 4.1). That is,

$$q_{E,S1964}^{ground}\left(\varepsilon_r\right) = 1.0741 \times q_{E,S1964}^{mixed}\left(\varepsilon_r\right) = 1.0741 \times \left(5.7604 - 0.63 \times \log_{10} \varepsilon_r\right)^2 \times 10^{-20}. \tag{B3}$$

B2 Number Density Fraction of Contamination

In Section B1, we assumed that the fraction of excited-state O^+ $f_{e/m}$ was 23% in the S1964 experiment. In this section, we detail the basis of this assumption. We first conclude that no measured fraction in existing studies is appropriate for direct application to the S1964 experiment. We then indirectly calibrate the S1964 results.

In laboratory ion beam experiments, the projectile O^+ is prepared by electron impact to O_2. Such electron impact creates both ground- and excited-state O^+ (Stebbings et al., 1966). The fraction depends on the energy of the ionizing electron. Table B1 summarizes reported fractions against electron energies.

S1964 created a projectile O^+ using the impact of 200-eV electrons colliding with O_2. They were unable to measure the fraction of O^+ states but they made "a crude estimate" that O^+ created by 200-eV electrons in their experiment includes 30% of the excited state. This estimate is based on private communication with J. W. McGowan, who observed the dependence of cross section on the ionizing electron energy.

Stebbings et al. (1966) provisionally measured the fraction of O^+ in the excited state using its dependence on the energy of the ionizing electron. The fraction was 34% for 50-eV electrons and 44% for 100-eV electrons. However, the fraction was not mentioned for 200-eV electrons used in S1964.

Turner et al. (1968) measured that the fraction of excited-state O^+ cross section was 27% for 50-eV electrons and 30% for 100-eV electrons. Turner et al. (1968) concluded that approximately one-third of the O^+ formed from O_2 by the electron impacts will be in excited states although they did not state the electron energy range for this conclusion. The fraction for 200-eV electrons (i.e., the energy used in S1964) is approximately 34% in their Figure 10, although they did not mention it.

However, this measurement with 200-eV electrons is likely unreliable as follows. Stebbings and Rutherford (1968) state that "Most of the measurements were carried out using 40-eV electrons" (p. 1037) and that "This energy was sufficiently low to ensure negligible production of O_2^{++}, which, if present, could not have been separated from O^+ in the analyzer." (p. 1037). We interpret this to mean that Stebbings and Rutherford (1968) were unable to clarify the fraction of O^+ in the excited state for 200 eV electrons that were used by S1964. The possible contamination of O_2^{++} is presumably the reason why there are no studies that discuss the 200-eV electrons used in S1964. Accordingly, we cannot directly calibrate the S1964 results.

In contrast, Stebbings and Rutherford (1968) concluded that the fraction of excited O^+ is 23% at 40 eV. This result appears established because Lindsay and Stebbings (2005) argue that their indirect estimation of 25%

Table B1
Fraction of Excited-State O^+ Contamination in Laboratory Experiment

	Energy of ionizing electron (eV)				
	Unstated[a]	40	50	100	200
Reference	Fraction of excited-state O^+				
Stebbings et al. (1964)	–	–	–	–	(30%)
Stebbings et al. (1966) Table 3	–	–	34%	44%	–
Stebbings and Rutherford (1968)	–	23%	–	–	–
Turner et al. (1968)	1/3	23%[b]	27%	30%	34%[b]
Rutherford and Vroom (1974)	–	–	–	–	–
Lindsay et al. (2001)	–	–	–	–	–
Lindsay and Stebbings (2005)	(25%)	–	–	–	–

Note. Number density fraction of the excited-state O^+ against total (excited and ground states). The fraction is sorted by the energies of electrons that were used to create O^+. Parentheses indicate that the value is not measured but discussed. Dashes indicate that fractions were not mentioned.
[a]The researchers did not state the corresponding energy range of the ionizing electron. [b]This value is not explicitly mentioned but can be seen in their Figure 10.

is entirely consistent with Stebbings and Rutherford (1968). Accordingly, it is possible to indirectly calibrate the S1964 results as follows.

Rutherford and Vroom (1974) measured the O^+-O cross section at 60–500 eV and concluded that their values are in good agreement with those of S1964 at 40–10,000 eV. Rutherford and Vroom (1974) presumably used 40-eV electrons to create O^+ as they did to create N^+. Thus, we can calculate the factor to calibrate the Rutherford and Vroom (1974) results and can apply the same factor to the S1964 results.

For clarification, the consistency between Stebbings et al. (1964) and Rutherford and Vroom (1974) is not readily clear because the adopted electron energies are different. One possibility is that the difference of fraction was small enough to affirm the consistency. Another possibility is that other detailed differences between the experiments tend to cancel the differences between fractions. For example, the experiment of Stebbings et al. (1964) is presumably also contaminated with O_2^{++} and excited-state neutral O atom, but that of Rutherford and Vroom (1974) is not (Lindsay & Stebbings, 2005; Stebbings & Rutherford, 1968). In other words, our calibration using the fraction of 23% does not necessarily imply that the fraction was exactly 23% in S1964 but may include other effects.

In summary, the fraction of excited-state O^+ is unknown for the S1964 cross section with 200-eV electrons. Thus, the S1964 cross section cannot be directly calibrated. However, the cross sections are numerically consistent between S1964 and Rutherford and Vroom (1974) (presumably with 40-eV electrons). Then, the S1964 model can be indirectly calibrated with a fraction of 23% at 40 eV (i.e., originally not for this model).

Data Availability Statement

Physical constants used in the present study are based on the 2018 Committee on Data for Science and Technology (CODATA) recommended values at https://physics.nist.gov/constants and the ninth edition of the international system of units (SI) brochure (2019) at https://www.bipm.org/.

Acknowledgments
A. Ieda would like to thank A. P. Hickman for helpful discussions. The author would like to thank Editage (www.editage.com) for English language editing. This work was supported by JSPS KAKENHI Grant 16K05568.

References

Adachi, K., Nozawa, S., Ogawa, Y., Brekke, A., Hall, C., & Fujii, R. (2017). Evaluation of a method to derive ionospheric conductivities using two auroral emissions (428 and 630 nm) measured with a photometer at Tromsø (69.6 degrees N). *Earth Planets and Space*, *69*, 90. https://doi.org/10.1186/s40623-017-0677-4

Anderson, C., Kosch, M. J., Nicolls, M. J., & Conde, M. (2013). Ion-neutral coupling in Earth's thermosphere, estimated from concurrent radar and optical observations above Alaska. *Journal of Atmospheric and Solar – Terrestrial Physics*, *105*, 313–324. https://doi.org/10.1016/j.jastp.2013.04.005

Banks, P. (1966). Collision frequencies and energy transfer—Ions. *Planetary and Space Science*, *14*(11), 1105–1122. https://doi.org/10.1016/0032-0633(66)90025-0

Banks, P. M., & Kockarts, G. (1973). *Aeronomy, Part A*. New York, NY: Academic Press.

Brekke, A. (2013). *Physics of the upper polar atmosphere* (2nd ed.). Heidelberg: Springer.

Brekke, A., & Hall, C. (1988). Auroral ionospheric quiet summer time conductances. *Annales Geophysicae-Atmospheres Hydrospheres and Space Sciences*, *6*(4), 361–375.

Buonsanto, M. J., Sipler, D. P., Davenport, G. B., & Holt, J. M. (1997). Estimation of the O^+–O collision frequency from coincident radar and Fabry-Perot observations at Millstone Hill. *Journal of Geophysical Research*, *102*(A8), 17267–17274. https://doi.org/10.1029/97ja01300

Burnside, R. G., Tepley, C. A., & Wickwar, V. B. (1987). The O^+–O collision cross-section: Can it be inferred from aeronomical measurements. *Annales Geophysicae*, *5A*(6), 343–349.

Capitelli, M., Lamanna, U. T., Guidotti, C., & Arrighini, G. P. (1977). The gerade-ungerade splitting of N_2^+ potentials: Effects on resonant charge transfer cross sections of nitrogen atoms. *Chemical Physics*, *19*(2), 269–278. https://doi.org/10.1016/0301-0104(77)85138-0

Carlson, H. C., & Harper, R. M. (1977). An experimental estimate of O^+–O resonant charge transfer cross section, collision frequency, and energy-transfer rate. *Journal of Geophysical Research*, *82*(7), 1144–1148. https://doi.org/10.1029/JA082i007p01144

COESA. (1976). *U.S. standard atmosphere, 1976*. Washington, DC: U.S. government printing office.

Dalgarno, A.. (1958a). Ambipolar diffusion in the F2-layer. *Journal of Atmospheric and Terrestrial Physics*, *12*(2,3), 219–220. https://doi.org/10.1016/0021-9169(58)90096-5

Dalgarno, A.. (1958b). The mobilities of ions in their parent gases. *Philosophical Transactions of the Royal Society of London – Series A: Mathematical and Physical Sciences*, *250*(982), 426–439. https://doi.org/10.1098/rsta.1958.0003

Dalgarno, A.. (1964). Ambipolar diffusion in the F-region. *Journal of Atmospheric and Terrestrial Physics*, *26*(9), 939. https://doi.org/10.1016/0021-9169(64)90236-3

Dalgarno, A., McDowell, M. R. C., & Williams, A. (1958). The mobilities of ions in unlike gases. *Philosophical Transactions of the Royal Society of London. Series A, Mathematical and Physical Sciences*, *250*(982), 411–425. https://doi.org/10.1098/rsta.1958.0002

Dang, T., Lei, J., Dou, X., & Wan, W. (2015). Feasibility study on the derivation of the O^+–O collision frequency from ionospheric field-aligned observations. *Journal of Geophysical Research: Space Physics*, *120*(7), 6029–6035. https://doi.org/10.1002/2015ja020987

Dyson, P. L., Davies, T. P., Parkinson, M. L., Reeves, A. J., Richards, P. G., & Fairchild, C. E. (1997). Thermospheric neutral winds at southern mid-latitudes: A comparison of optical and ionosonde h_mF_2 methods. *Journal of Geophysical Research*, *102*(A12), 27189–27196. https://doi.org/10.1029/97ja02138

Fang, T.-W., Anderson, D., Fuller-Rowell, T., Akmaev, R., Codrescu, M., Millward, G., et al. (2013). Comparative studies of theoretical models in the equatorial ionosphere. In J. Huba, R. Schunk, & G. Khazanov (Eds.), Modeling the ionosphere-thermosphere system, geophysical monograph series (Vol. *201*, pp. 133–144). Washington, DC: American Geophysical Union. https://doi.org/10.1002/9781118704417.ch12

Heiche, G., & Mason, E. A. (1970). Ion mobilities with charge exchange. *The Journal of Chemical Physics*, *53*(12), 4687–4696. https://doi.org/10.1063/1.1673997

Hickman, A. P., Medikeri-Naphade, M., Chapin, C. D., & Huestis, D. L. (1997a). Fine structure effects in the O^+–O collision frequency. *Geophysical Research Letters*, *24*(2), 119–122. https://doi.org/10.1029/96gl03797

Hickman, A. P., Medikeri-Naphade, M., Chapin, C. D., & Huestis, D. L. (1997b). Calculation of fine-structure effects in O^+–O collisions. *Physical Review A*, *56*(6), 4633–4643. https://doi.org/10.1103/PhysRevA.56.4633

Ieda, A. (2020). Ion-neutral collision frequencies for calculating ionospheric conductivity. *Journal of Geophysical Research: Space Physics*, *125*, e2019JA027128. https://doi.org/10.1029/2019JA027128

Ieda, A., Oyama, S., Vanhamäki, H., Fujii, R., Nakamizo, A., Amm, O., et al. (2014). Approximate forms of daytime ionospheric conductance. *Journal of Geophysical Research: Space Physics*, *119*(12), 10397–10415. https://doi.org/10.1002/2014ja020665

Joshi, P. P., Waldrop, L. S., & Brum, C. G. M. (2018). Ionospheric O^+ momentum balance through charge exchange with thermospheric O atoms. *Journal of Geophysical Research: Space Physics*, *123*(11), 9743–9761. https://doi.org/10.1029/2018ja025821

Kelley, M. C. (2009). *Earth's ionosphere: Plasma physics and electrodynamics* (2nd ed.). London: Elsevier.

Kiene, A., Bristow, W. A., Conde, M. G., & Hampton, D. L. (2019). High-resolution local measurements of F region ion temperatures and Joule heating rates using SuperDARN and ground-based optics. *Journal of Geophysical Research: Space Physics*, *124*(1), 557–572. https://doi.org/10.1029/2018ja025997

Knof, H., Mason, E. A., & Vanderslice, J. T. (1964). Interaction energies, charge exchange cross sections, and diffusion cross sections for N^+–N and O^+–O collisions. *The Journal of Chemical Physics*, *40*(12), 3548–3553. https://doi.org/10.1063/1.1725050

Lindsay, B. G., Sieglaff, D. R., Smith, K. A., & Stebbings, R. F. (2001). Charge transfer of keV O^+ ions with atomic oxygen. *Journal of Geophysical Research*, *106*(A5), 8197–8203. https://doi.org/10.1029/2000ja000437

Lindsay, B. G., & Stebbings, R. F. (2005). Charge transfer cross sections for energetic neutral atom data analysis. *Journal of Geophysical Research*, *110*(A12), A12213. https://doi.org/10.1029/2005ja011298

Lomidze, L., Scherliess, L., & Schunk, R. W. (2015). Magnetic meridional winds in the thermosphere obtained from Global Assimilation of Ionospheric Measurements (GAIM) model. *Journal of Geophysical Research: Space Physics*, *120*(9), 8025–8044. https://doi.org/10.1002/2015ja021098

Mason, E. A., & Vanderslice, J. T. (1959). Mobility of hydrogen ions (H^+,H_2^+,H_3^+) in hydrogen. *Physical Review*, *114*(2), 497–502. https://doi.org/10.1103/PhysRev.114.497

McDonald, S. E., Lean, J. L., Huba, J. D., Joyce, G., Emmert, J. T., & Drob, D. P. (2013). Long-term simulations of the ionosphere using SAMI3. In J. Huba, R. Schunk, & G. Khazanov (Eds.), Modeling the ionosphere-thermosphere system, geophysical monograph series (Vol. *201*, pp. 119–131). Washingon, DC: American Geophysical Union. https://doi.org/10.1002/9781118704417.ch11

McGranaghan, R., Knipp, D. J., Solomon, S. C., & Fang, X. (2015). A fast, parameterized model of upper atmospheric ionization rates, chemistry, and conductivity. *Journal of Geophysical Research: Space Physics*, *120*(6), 4936–4949. https://doi.org/10.1002/2015ja021146

Nicolls, M. J., Aponte, N., Gonzalez, S. A., Sulzer, M. P., & Oliver, W. L. (2006). Daytime F region ion energy balance at Arecibo for moderate to high solar flux conditions. *Journal of Geophysical Research*, *111*(A10), A10307. https://doi.org/10.1029/2006ja011664

Oliver, W. L., & Glotfelty, K. (1996). O^+–O collision cross section and long-term F region O density variations deduced from the ionospheric energy budget. *Journal of Geophysical Research*, *101*(A10), 21769–21784. https://doi.org/10.1029/96ja01585

Partridge, H., & Stallcop, J. R. (1986). N+–N and O+–O interaction energies, dipole transition moments, and transport cross sections. In J. N. Moss & C. D. Scott (Eds.), AIAA Progress in astronautics and aeronautics: Thermophysical aspects of re-entry flows (Vol. *103*, pp. 243–260). New York, NY: AIAA.

Pesnell, W. D., Omidvar, K., & Hoegy, W. R. (1993). Momentum-transfer collision frequency of O^+–O. *Geophysical Research Letters*, *20*(13), 1343–1346. https://doi.org/10.1029/93gl01597

Pesnell, W. D., Omidvar, K., Hoegy, W. R., & Wharton, L. E. (1994). O^+–O collision frequency in high-speed flows. *Journal of Geophysical Research*, *99*(A11), 21375–21382. https://doi.org/10.1029/94ja01650

Rutherford, J. A., & Vroom, D. A. (1974). The reaction of atomic oxygen with several atmospheric ions. *The Journal of Chemical Physics*, *61*(7), 2514–2519. https://doi.org/10.1063/1.1682371

Salah, J. E. (1993). Interim standard for the ion-neutral atomic oxygen collision frequency. *Geophysical Research Letters*, *20*(15), 1543–1546. https://doi.org/10.1029/93gl01699

Schunk, R. W., & Nagy, A. F. (2009). *Ionospheres: Physics, plasma physics, and chemistry* (2nd ed.). New York, NY: Cambridge University Press.

Schunk, R. W., & Walker, J. C. G. (1973). Theoretical ion densities in lower ionosphere. *Planetary and Space Science*, *21*(11), 1875–1896. https://doi.org/10.1016/0032-0633(73)90118-9

Stallcop, J. R. (1971). N_2^+ potential-energy curves. *The Journal of Chemical Physics*, *54*(6), 2602–2605. https://doi.org/10.1063/1.1675218

Stallcop, J. R., Levin, E., & Partridge, H. (1998). Transport properties of hydrogen. *Journal of Thermophysics and Heat Transfer*, *12*(4), 514–519. https://doi.org/10.2514/2.6370

Stallcop, J. R., & Partridge, H. (1985). N^+–N long-range interaction energies and resonance charge exchange. *Physical Review A*, *32*(1), 639–642. https://doi.org/10.1103/PhysRevA.32.639

Stallcop, J. R., Partridge, H., & Levin, E. (1991). Resonance charge transfer, transport cross sections, and collision integrals for $N^+(^3P)$–$N(^4S^0)$ and $O^+(^4S^0)$–$O(^3P)$ interactions. *The Journal of Chemical Physics*, *95*(9), 6429–6439. https://doi.org/10.1063/1.461563

Stebbings, R. F., & Rutherford, J. A. (1968). Low-energy collisions between $O^+(^4S)$ and H(1s). *Journal of Geophysical Research*, *73*(3), 1035–1038. https://doi.org/10.1029/JA073i003p01035

Stebbings, R. F., Smith, A. C. H., & Ehrhardt, H. (1964). Charge transfer between oxygen atoms and O^+ and H^+ ions. *Journal of Geophysical Research*, *69*(11), 2349–2355. https://doi.org/10.1029/JZ069i011p02349

Stebbings, R. F., Turner, B. R., & Rutherford, J. A. (1966). Low-energy collisions between some atmospheric ions and neutral particles. *Journal of Geophysical Research*, *71*(3), 771–784. https://doi.org/10.1029/JZ071i003p00771

Stubbe, P. (1968). Frictional forces and collision frequencies between moving ion and neutral gases. *Journal of Atmospheric and Terrestrial Physics*, *30*(12), 1965–1985. https://doi.org/10.1016/0021-9169(68)90004-4

Takeda, M. (2016). Long-term variation of Ampère force by geomagnetic *Sq* currents and thermospheric pressure difference. *Journal of Geophysical Research: Space Physics*, *121*(11), 11407–11412. https://doi.org/10.1002/2016ja022845

Turner, B. R., Rutherford, J. A., & Compton, D. M. J. (1968). Abundance of excited ions in O^+ and O_2^+ ion beams. *The Journal of Chemical Physics*, *48*(4), 1602–1608. https://doi.org/10.1063/1.1668882

Vickers, H., Kosch, M. J., Sutton, E., Ogawa, Y., & La Hoz, C. (2013). Thermospheric atomic oxygen density estimates using the EISCAT Svalbard Radar. *Journal of Geophysical Research: Space Physics*, *118*(3), 1319–1330. https://doi.org/10.1002/jgra.50169

Wu, Q., Wang, W., Roble, R. G., Häggström, I., & Strømme, A. (2012). First daytime thermospheric wind observation from a balloon-borne Fabry-Perot interferometer over Kiruna (68N). *Geophysical Research Letters*, *39*, L14104. https://doi.org/10.1029/2012gl052533

Zossi, B. S., Fagre, M., & Elias, A. G. (2019). Pedersen ionic contribution in different time scales. *Journal of Geophysical Research: Space Physics*, *124*(8), 6961–6970. https://doi.org/10.1029/2019ja026884